



ARTICLE

# Harnessing a methane-fueled, sediment-free mixed microbial community for utilization of distributed sources of natural gas

Jeffrey J. Marlow<sup>1</sup>  | Amit Kumar<sup>1,2,†</sup> | Brandon C. Enalls<sup>1</sup>  |  
Linda M. Reynard<sup>3</sup> | Noreen Tuross<sup>3</sup> | Gregory Stephanopoulos<sup>2</sup> | Peter Girguis<sup>1</sup>

<sup>1</sup> Department of Organismic and Evolutionary Biology, Harvard University, Cambridge, Massachusetts

<sup>2</sup> Department of Chemical Engineering, Massachusetts Institute of Technology, Cambridge, Massachusetts

<sup>3</sup> Department of Human Evolutionary Biology, Harvard University, Cambridge, Massachusetts

## Correspondence

Gregory Stephanopoulos, 77 Massachusetts Ave. 56-469 Cambridge, MA, 02139.

Email: gregstep@mit.edu

Peter Girguis, 16 Divinity Ave., Biological Laboratories Building, 3083 Cambridge, MA, 020138-2020.

Email: pgirguis@oeb.harvard.edu

## Funding information

Advanced Research Projects Agency – Energy,

Grant number: DE-AR0000433; The U.S.

National Science Foundation, Grant number:

DEB-1542506

## Abstract

Harnessing the metabolic potential of uncultured microbial communities is a compelling opportunity for the biotechnology industry, an approach that would vastly expand the portfolio of usable feedstocks. Methane is particularly promising because it is abundant and energy-rich, yet the most efficient methane-activating metabolic pathways involve mixed communities of anaerobic methanotrophic archaea and sulfate reducing bacteria. These communities oxidize methane at high catabolic efficiency and produce chemically reduced by-products at a comparable rate and in near-stoichiometric proportion to methane consumption. These reduced compounds can be used for feedstock and downstream chemical production, and at the production rates observed in situ they are an appealing, cost-effective prospect. Notably, the microbial constituents responsible for this bioconversion are most prominent in select deep-sea sediments, and while they can be kept active at surface pressures, they have not yet been cultured in the lab. In an industrial capacity, deep-sea sediments could be periodically recovered and replenished, but the associated technical challenges and substantial costs make this an untenable approach for full-scale operations. In this study, we present a novel method for incorporating methanotrophic communities into bioindustrial processes through abstraction onto low mass, easily transportable carbon cloth artificial substrates. Using Gulf of Mexico methane seep sediment as inoculum, optimal physicochemical parameters were established for methane-oxidizing, sulfide-generating mesocosm incubations. Metabolic activity required  $>\sim 40\%$  seawater salinity, peaking at 100% salinity and 35 °C. Microbial communities were successfully transferred to a carbon cloth substrate, and rates of methane-dependent sulfide production increased more than threefold per unit volume. Phylogenetic analyses indicated that carbon cloth-based communities were substantially streamlined and were dominated by *Desulfotomaculum geothermicum*. Fluorescence in situ hybridization microscopy with carbon cloth fibers revealed a novel spatial arrangement of

<sup>†</sup>Current address: Department of Mechanical Engineering, Massachusetts Institute of Technology, Cambridge, MA 02139.

Jeffrey J. Marlow and Amit Kumar contributed equally to this work.

This is an open access article under the terms of the Creative Commons Attribution-NonCommercial-NoDerivs License, which permits use and distribution in any medium, provided the original work is properly cited, the use is non-commercial and no modifications or adaptations are made.

© 2018 The Authors. *Biotechnology and Bioengineering* Published by Wiley Periodicals Inc.

anaerobic methanotrophs and sulfate reducing bacteria suggestive of an electronic coupling enabled by the artificial substrate. This system: 1) enables a more targeted manipulation of methane-activating microbial communities using a low-mass and sediment-free substrate; 2) holds promise for the simultaneous consumption of a strong greenhouse gas and the generation of usable downstream products; and 3) furthers the broader adoption of uncultured, mixed microbial communities for biotechnological use.

#### KEYWORDS

anaerobic oxidation of methane, biofuel production, carbon cloth artificial substrate, greenhouse gas mitigation

## 1 | INTRODUCTION

The use of methane in the production of infrastructure-compatible, industrially relevant products is an attractive prospect with benefits of energy generation, chemical production, and climate regulation. The production of natural gas, which is composed primarily of methane, has reached historically high rates (U.S. Energy Information Administration, 2016). This trend provides affordable feedstock on a global scale, much of which is produced by small, distributed units that are not well-served by energy-intensive chemical plants that require high capital infrastructure expenditures (Clomburg, Crumbley, & Gonzalez, 2017; Emerson et al., 2017). In addition, leakage associated with natural gas production delivers tens of teragrams of methane to the atmosphere each year (Brandt et al., 2014). Given methane's strength as a greenhouse gas, minimizing this loss is a key priority of climate change mitigation strategies (Howarth, 2014; Stocker, 2014).

While synthetic catalysts have shown promise in methane reforming (York, Xiao, & Green, 2003)—particularly through high-temperature transformations (Takenaka, Kobayashi, Ogihara, & Otsuka, 2003; Tang, Zhu, Wu, & Ma, 2014)—biological processes are particularly compelling given their more moderate operating conditions, highly selective methane-activating biochemistry, and self-sustaining maintenance. A microbial system's ability to perform several transformations within a small volume minimizes complexity and cost of multi-step conversions (Clomburg, Crumbley, & Gonzalez, 2017).

The anaerobic oxidation of methane (AOM) is an energy- and carbon-efficient process with a near-catalytic processivity: only 1–3% of methane-carbon enters cell biomass (Nauhaus, Albrecht, Elvert, Boetius, & Widdel, 2007; Treude et al., 2007). In contrast, aerobic methanotrophy proceeds at faster rates, but sequesters a higher proportion of methane-derived carbon as biomass (Hanson & Hanson, 1996) and has a lower energy efficiency and higher reactant costs (Haynes & Gonzalez, 2014; Trotsenko & Murrell, 2008). AOM with sulfate as an electron acceptor is typically mediated by syntrophic consortia of anaerobic methanotrophic archaea (ANME) and sulfate reducing bacteria (SRB) that are abundant in anoxic sediments at marine methane seeps (Boetius et al., 2000; Ruff et al., 2015). Their

slow growth (Girguis, Cozen, & DeLong, 2005; Krüger, Wolters, Gehre, Joye, & Richnow, 2008) and remarkable resistance to laboratory culture isolation make ANME-SRB consortia challenging constituents of industrial processes.

Despite these apparent obstacles, AOM metabolism holds substantial promise for the efficient conversion of a strong greenhouse gas into high-value products. Attempts to incorporate AOM into a cultivable methanogen have produced a *M. acetivorans* strain with an ANME-1 *mcr* gene that uses ferric iron as an electron acceptor (Soo et al., 2016) and whose modeled capabilities include methanol, ethanol, butanol, and isobutanol production (Nazem-Bokaei, Gopalakrishnan, Ferry, Wood, & Maranas, 2016). The addition of a 3-hydroxybutyryl-CoA dehydrogenase gene from *C. acetobutylicum* enabled lactate formation (McAnulty et al., 2017). These important contributions would be complemented by sulfate-coupled methane-oxidizing industrial capabilities, whereby diffusible, environmentally abundant electron acceptors could help generate easily transportable liquid-phase products. Moreover, there are clear advantages of working with mixed communities; in comparison to pure cultures, diverse assemblages of organisms are more resilient to environmental perturbations and offer a substantially wider range of functional capabilities (Briones & Raskin, 2003; Girvan, Campbell, Killham, Prosser, & Glover, 2005).

Here, we report a method for sustaining methane-oxidizing, sulfide-generating communities on artificial substrates that can be maintained without frequent re-inoculation from deep-sea sediments. This approach offers several industrial benefits, both in its current configuration and as an enabling technology for future enhancements. By converting methane to dissolved inorganic carbon, greenhouse warming potential is reduced more than an order of magnitude (Stocker, 2014), and engineered autotrophs could be introduced downstream to generate high-value liquid fuels (Claassens, Sousa, dos Santos, de Vos, & Van der Oost, 2008; Lan & Liao, 2013). In addition to building a symbiosis with ANME to enable methane consumption, sulfate-reducing bacteria can remediate heavy metals (García, Moreno, Ballester, Blázquez, & González, 2001; Joo, Choi, Kim, Kim, & Oh, 2015) and produce plastic precursor storage molecules (Hai, Lange,

Rabus, & Steinbüchel, 2004; Wang, Yin, & Chen, 2014). Sulfide generated through this process can be used as feedstock for genetically tractable chemoautotrophs (Kernan, West, & Banta, 2017; Nybo, Khan, Woolston, & Curtis, 2015), which can make high-value chemical products (Kernan et al., 2016). Finding a conductive physical scaffold to enable industrially-relevant reactions within the context of an ecophysiological sustainable system—whereby microbial communities can take advantage of natural electrical and chemical gradients (e.g., Pfeffer et al., 2012)—would decrease transport and scale-up costs while building a robust, customizable system. Furthermore, methane seep microbial communities can withstand relatively high concentrations of sulfide, a prominent contaminant of natural gas reservoirs (Faramawy, Zaki, & Sakr, 2016; Sublette & Sylvester, 1987), obviating the costly process of feedstock purification and opening large quantities of “dirty methane” to bioindustrial use.

To inform the conditions needed for the initial biochemical transformations in this multipartite system, we identify salinity and temperature conditions needed for optimized methane consumption in natural sediment mesocosms, and evaluate the changes in microbial community structure associated with heightened methane consumption and sulfide production rates. Ultimately, we demonstrate robust sediment-free AOM activity on a conductive, high-surface area artificial substrate that promotes enhanced methane activation and sulfide production via a streamlined microbial community. These methanotrophic biocatalytic systems are poised to provide economically viable solutions for liquid fuel or chemical production.

## 2 | MATERIALS AND METHODS

### 2.1 | Seep sediment collection and handling

Seep sediment was collected from Mississippi Canyon (MC) lease block 036 (28°56′05.1″N, 88°11′50.4″ W) as a part of the *Alvin* Science Verification Cruise aboard *R/V Atlantis* leg AT 26-12 to the Gulf of Mexico in March, 2014. MC is well established as a site of methane and hydrocarbon seepage (Coffin et al., 2008; Lloyd et al., 2010; Shank et al., 2012). Push cores (PC) 6 and 9 were collected from white microbial mat, ~30 cm apart from each other. Upon recovery, sediment was divided into 3 cm horizons and placed in sterile whirlpak bags, which were then stored in Ar-sparged Mylar bags at 4 °C until later use. This approach is effective at keeping sediment-hosted communities viable and has been used for many studies of seep-associated activity (Beal, Claire, & House, 2011; Pasulka et al., 2016). Two weeks prior to use in incubation experiments, sediment was mixed 1:1 v/v with 0.22 μm-filtered seawater to make sediment slurry, which was placed in an autoclaved bottle, sparged with CH<sub>4</sub>, and kept at 4 °C.

### 2.2 | Salinity experiment set-up

Eight treatments of different salinity conditions were set up, in triplicate, using homogenized sediment from the 3–12 cm horizon of PC6. To adjust salinity levels, sediment samples were centrifuged

(4,500 rcf, 8 min), supernatant was removed, and an equivalent volume of freshwater medium (Stams, Van Dijk, Dijkema, & Plugge, 1993) was added. The mixture was vortexed, and salinity levels were measured using a calibrated B-771 LAQUAtwin conductivity meter (Horiba Instruments, Irvine, CA). Sulfate was added to each condition to reach full seawater levels; concentrations were confirmed using the BaCl method (Kolmert, Wikström, & Hallberg, 2000). For each condition, 40 ml of sediment slurry were distributed to triplicate 120 ml autoclaved glass vials. Vials were sparged with N<sub>2</sub> and then CH<sub>4</sub> gas for 5 min each. A total of 80 ml of CH<sub>3</sub>D were added to an overall pressure of two atm, and vials were placed in a 4 °C cold room. Anoxic conditions were maintained throughout.

### 2.3 | Temperature experiment set-up

Eight milliliters of homogenized sediment slurry from the 3–15 cm horizon of PC9 were distributed into autoclaved 27-ml balch tubes for each experimental condition at 5.5, 20, 35, and 50 °C. Each temperature condition included a triplicate set with CH<sub>4</sub> headspace (following 5 min of CH<sub>4</sub> sparging) and a triplicate set with N<sub>2</sub> headspace (following 5 min of N<sub>2</sub> sparging); the 5.5 °C condition also included a killed control triplicate set with CH<sub>4</sub> sparging and headspace. Tubes were kept (unshaken) in incubators at the designated temperatures throughout the experiment.

### 2.4 | Artificial substrate experiment set-up

To transfer sediment-hosted microbial constituents to artificial substrates, the following procedure was used. In an anoxic chamber (Coy Laboratory Products, maintained at <3 ppm O<sub>2</sub> and 2.6% H<sub>2</sub>), balch tubes were opened, autoclave-sterilized substrates (~6 cm<sup>3</sup>) were inserted and mixed with the sediment slurry (PC9), and tubes were re-capped. Outside of the chamber, the slurry was sparged with CH<sub>4</sub> for 5 min and placed back in the temperature-appropriate incubator. After 2 weeks, the substrates were removed and transferred to a sterile tube with 12 ml of 0.22 μm-filtered seawater (all steps performed in the anoxic chamber). This transfer process was repeated five more times, and final incubation tubes contained no visible sediment.

Two artificial substrates were used in AOM incubation experiments: carbon cloth (CarboCloth, buyactivatedcharcoal.com, Crawford, NE, \$42/L-incubation) and yttria stabilized zirconium oxide beads (zircon beads hereafter; MSE Supplies, Tucson, AZ, \$335/L-incubation). Both substances are suitable for industrial use, as they are chemically inert, non-toxic, and are available in bulk volumes (see suppliers' websites for additional specifications).

In experiments evaluating differences in biomass association with carbon cloth and polyurethane filters, 30 ml of PC9 sediment slurry was added to sterilized 60 ml vials. In one triplicate set, 5 ml of carbon cloth was inserted into each vial; in a different triplicate set, 5 ml of polyurethane filter (Hagen Corp., Mansfield, MA) was used. Vials were set up in the anoxic chamber, capped, and sparged with N<sub>2</sub> and CH<sub>4</sub> for 5 min each before being overpressured at two atm with methane gas.

In both cases, artificial substrate was pre-autoclaved, and one methane-free control was established. After 27 days, substrates were removed for cell counts.

## 2.5 | Sulfide concentration

Sulfide concentrations were quantified using the Cline assay (Cline, 1969), as described previously (Scheller, Yu, Chadwick, McGlynn, & Orphan, 2016). Briefly, supernatant was removed in an anoxic chamber by syringe through the stopper, and pushed through a 0.22  $\mu\text{m}$  filter (Durapore, EMD Millipore). A total of 500  $\mu\text{l}$  of filtered supernatant was mixed with 500  $\mu\text{l}$  of 500 mM zinc acetate. A total of 200  $\mu\text{l}$  of this mixture was added, in triplicate, to microplate wells. A total of 20  $\mu\text{l}$  of a 1:1 mixture of 30 mM  $\text{FeCl}_3 \times 6\text{H}_2\text{O}$  in 6N HCl and 11.5 mM N,N-dimethyl-p-phenylenediamine dihydrochloride in 6N HCl was added to each well. After 1 hr at room temperature, absorbance at 670 nm was measured using a Spectramax i3 multi-mode microplate detection platform. Medium-specific standards and blanks were made to generate absorbance–concentration relationships.

## 2.6 | Methane oxidation rates

Rates of methane oxidation were calculated using the monodeuterated methane approach detailed previously (Marlow et al., 2017), in which oxidative reactions lead to elevated quantities of deuterium in the aqueous phase. A LGR DLT-100 liquid water isotope analyzer (LWIA, Los Gatos Research, CA) was used to determine the D/H ratio of each sample. Increased D/H ratios indicate methane activation rather than full methane oxidation, but consistent scaling factors equating D/H values with full methane oxidation (as calibrated with the well established  $^{14}\text{C}$  radiolabel approach) allow for precise, reliable rate measurements (Marlow et al., 2017).

## 2.7 | 16S rRNA gene sequencing and diversity analysis

DNA from approximately 0.5 g (wet weight) sediment (time-zero sediment and all four temperature conditions, in triplicate for 5 and 35  $^{\circ}\text{C}$ ) or carbon cloth (in triplicate for the 35  $^{\circ}\text{C}$  samples) was extracted as previously described (Girguis, Orphan, Hallam, & DeLong, 2003). The extraction protocol was modified by bead beating and incubating the samples twice upon addition of the lysis buffer. Extract was purified of inhibitors using the Aurora system (Boreal Genomics, Vancouver, BC) Clean Up Protocol and PCR validated using 27F and 1492R primers (Weisburg, Barns, Pelletier, & Lane, 1991). The PCR included denaturation at 94  $^{\circ}\text{C}$  for 5'; 35 cycles of 94  $^{\circ}\text{C}$  for 40", 55  $^{\circ}\text{C}$  for 40", and 68  $^{\circ}\text{C}$  for 2'; and a final extension at 68  $^{\circ}\text{C}$  for 5'. PCR products were separated by gel electrophoresis; template-free negative controls exhibited no visible amplified product. Amplified DNA was sequenced on an Illumina MiSeq platform (10,000 300 bp paired-end reads per assay) by Research and Testing Laboratory (Lubbock, TX) targeting the V4 region of the 16S rRNA gene using the

515F and 806R Earth Microbiome Project primers (Caporaso et al., 2011, 2012). Denoising, chimera checking, quality benchmarking, OTU clustering using UPARSE (Edgar, 2013), and USEARCH (Edgar, 2010) alignment against NCBI-database sequences was performed according to the RTL Data Analysis Methodology document (RTL Genomics, 2016).

The Chao-1 alpha diversity parameter was calculated as reported elsewhere (Chao, 1984; Colwell & Coddington, 1994). Inverse Simpson values ( $1/\lambda$ ) were calculated by first determining Simpson's index ( $\lambda$ ) using equation 1,

$$\lambda = \frac{\sum_{j=1}^s n_j (n_j - 1)}{N(N - 1)} \quad (1)$$

where  $n_j$  is the number of sequences recovered of the  $j$ th OTU,  $N$  is the overall number of sequences, and  $s$  is the number of observed OTUs (Hunter & Gaston, 1988; Simpson, 1949).

## 2.8 | Cell counts

Cell counts were performed as described previously (Marlow, Steele, Case, et al., 2014), with minor adjustments. For one replicate from each temperature-substrate combination, 0.5 ml of substrate and 0.5 ml of liquid medium were collected at the incubation end point (1 ml of well-mixed slurry was used for the seep sediment samples) and fixed in 2% paraformaldehyde for 1 hr. For artificial substrate samples, supernatant was separated from substrate and, for carbon cloth and zircon bead 44-day incubations, analyzed separately. A total of 1 ml of 0.22  $\mu\text{m}$  filtered PBS was added to the artificial substrates in 2 ml tubes. Sediment slurry and artificial substrate tubes were subjected to sonication on ice to recover substrate-bound cells (5  $\times$  8 s, 5–6 W, using a Thermo Fisher Scientific, Waltham, MA Model F60 sonicator); subsequent microscopy of all substrates demonstrated that  $> \sim 96\%$  of biomass had been recovered by sonication. 0.5 ml of Percoll (Sigma-Aldrich, St. Louis, MO) was added, and tubes were centrifuged at 4,800 rpm for 15 min at 4  $^{\circ}\text{C}$ . Unpelleted material was concentrated on a 0.22  $\mu\text{m}$  white polycarbonate filter (Millipore), and 2 ml of PBS was used to rinse the filters. Fluorescence in situ hybridization (FISH) was performed on select filters, and the general DNA stain DAPI was applied ( $\sim 25 \mu\text{l}$  per filter). Filters were examined with a Zeiss Axio Scope A1 under a 50 $\times$  objective; cells were counted across 15 fields of view, and calculations were based on grid area, total filter area, and volume of starting material.

## 2.9 | Fluorescence in situ hybridization and microscopy

For in-place analysis of intact substrates (sediment, carbon cloth, and polyurethane filter), approximately 0.5 g of each substrate was removed from its respective tube, fixed in 4% paraformaldehyde overnight at 4  $^{\circ}\text{C}$ , and washed in 2 min sequential incubations of 50%, 80%, and 90% ethanol (balance PBS). FISH was performed on intact substrates and filters (prepared as in the "Cell Counts" section above)

as described in Dekas, Poretsky, and Orphan, (2009) using the following probes (Biomers, Ulm, Germany) at final concentrations of 5 ng/ $\mu$ l: ANME-932 (5'-AGCTCACCCGTTGAGT-3'; Boetius et al., 2000) with a 5' conjugated Cyanine 3 dye and 50% formamide, and DSS-658 (5'-TCCACTCCCTCTCCCAT-3'; Manz, Eisenbrecher, Neu, & Szewzyk, 1998) with a 5' conjugated 6-FAM dye and 60% formamide. Negative control cultures of *E. coli* and *M. marburgensis* were used to detect any non-specific probe binding (none was observed). Samples were placed on glass slides, and incubated with hybridization buffer in closed Falcon tubes at 46 °C for 12 hr. Slides were then immersed in pre-warmed wash buffer for 15 min at 48 °C, rinsed with DI water, and allowed to air dry. Samples were analyzed with a Zeiss LSM 880 Inverted Confocal microscope using lasers at wavelengths 488 nm and 561 nm; a reflectance channel recorded 80% of the reflection from the 488 nm laser. Laser power, scan rates, and gain settings were set to minimize background signal. Images were acquired with the ZEN software.

## 2.10 | Electrical resistance

Resistance was measured using the 117 True RMS Multimeter (Fluke, Everett, WA). Five point measurements were obtained from random portions of each substrate with probes separated by 2 cm, and mean and standard deviation values were calculated.

## 3 | RESULTS AND DISCUSSION

### 3.1 | Medium composition and influence of salinity on methanotrophic activity

ANME-SRB consortia are most abundant and active in marine sediments perfused with upward-advecting reduced fluids and downward circulating sulfate-rich seawater (Joye et al., 2004; Treude et al., 2003). We sought to determine if AOM activity could be retained under low-salt conditions, as reduced salinity may be desirable in select biotechnology applications.

Triplicate mesocosm incubations of seep sediment were established at 4 °C under conditions of varying salinity but constant sulfate concentrations (to maintain a consistent Gibbs free energy value; Supplementary Table S1). Methane oxidation was measurable only in samples with salinities greater than ~2.2 wt% salt (22 g/kg, or ~63% seawater salinity; Figure 1). Full-salinity samples oxidized methane at a rate of 138 (+/- 18.4) nmol/cm<sup>3</sup> d after 245 days, while the 63% salinity incubations exhibited 32% (+/- 8.5%) as much activity. These values are consistent with previously characterized seep substrates (Marlow, Steele, Ziebis, et al., 2014; Treude et al., 2003; Wegener et al., 2008). The absence of detectable methane oxidation in other conditions—samples with 17–39% salinity levels and full-salinity killed control incubations—suggests that a threshold of >~40% seawater salinity (e.g., 15.8 ms/cm) is required for AOM activity. This threshold is likely closer to 45% if the observed decrease in methane oxidizing activity with lower salinity is governed by a linear relationship. The use of constant sulfate concentrations (~28 mM) means that the energetic driving force of AOM was not a distinguishing factor.

ANME-SRB-mediated AOM results in a 1:1 stoichiometry of methane oxidation and sulfate reduction (Boetius et al., 2000), but alternative electron donors can facilitate sulfate reduction in seafloor sediments (Kleindienst et al., 2014) and decouple this 1:1 relationship. In our experiments, sulfide production exceeded methane consumption: using the 245-day time points of the 100% and 63% salinity incubations, AOM accounted for 74% and 71% of sulfide production, respectively. Sulfide production was not observed at 20% salinity but did occur in the absence of methane activation at 39% and 28% salinity (Figure 1). These data demonstrate that sulfate reducing organisms in our mesocosm incubations can use non-methane electron donors and are less affected by—but still subject to—challenges associated with low salinity.

Our data demonstrate that Gulf of Mexico seep sediment-derived communities require full seawater levels of salinity to attain optimal activity. While this finding is consistent with the marine environment from which the inoculum was collected, a physiological explanation remains to be determined. Freshwater AOM has typically been associated with non-sulfate electron acceptors such as nitrate (Deutzmann & Schink, 2011; Smemo & Yavitt, 2007), and previous observations of freshwater sulfate-reducing AOM reported substantially lower rates (~8 nmol/cm<sup>3</sup> day; Timmers et al., 2016). Some methanogens require seawater-level salinity, potentially to maintain cell ultrastructure (Kadam, Ranade, Mandelco, & Boone, 1994). Energetics-based effects of salinity on metabolism—potentially associated with electrical conductivity (Wegener, Krukenberg, Riedel, Tegetmeyer, & Boetius, 2015) or osmoregulation (Csonka & Hanson, 1991)—warrant further investigation.

### 3.2 | Influence of temperature on sulfate reduction activity by seep sediment communities

To determine if AOM-coupled sulfide production could be enhanced at elevated temperatures, we measured sulfide production under high-methane, full seawater salinity conditions at 5, 20, 35, and 50 °C. Triplicate incubations of Gulf of Mexico sediment (recovered from ~5 °C sediments) were evaluated for 72 days, and measured sulfide concentrations were used as a proxy for methane oxidation (Figure 2). As described above, sulfide production rates were consistently proportional to methane oxidation rates in experiments using co-localized seep sediment inoculum (0.71–0.74 methane oxidized: sulfate reduced, Figure 1).

Sulfide production rates were highest at 35 °C: this condition yielded ~18.6 nmol/cm<sup>3</sup> day over the first 44 days of the experiment, corresponding to 13.8 nmol methane oxidation/cm<sup>3</sup> day (calculated using a sulfide production-to-methane oxidation scaling factor of 0.74 from the full-salinity incubations). This value is substantially lower than the methane oxidation rate of the full-salinity condition described above, likely due to localized heterogeneity of seep sediments (Marlow, Steele, Case, et al., 2014; Orphan et al., 2004) and the “dilution” effect of using a broader horizon of sediment beyond the standard sulfate-methane transition zone (Joye et al., 2004; Lloyd et al., 2010). Sulfide production rates in the 50 °C incubations were

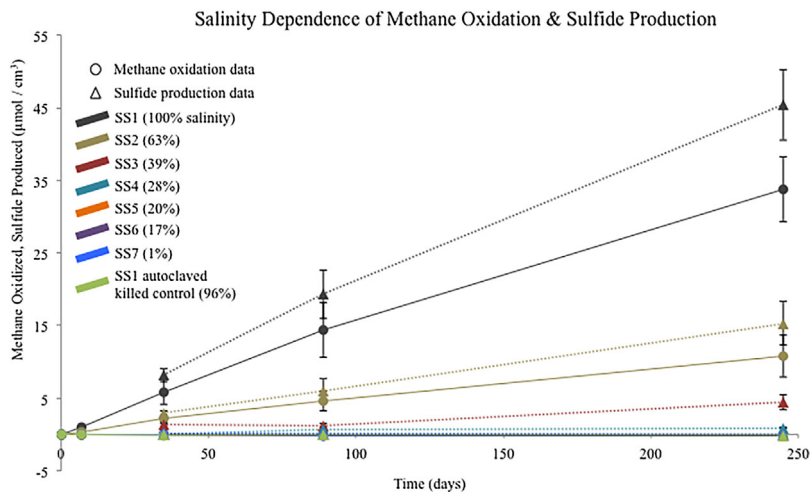


**FIGURE 1** Concentrations of methane oxidized and sulfide produced in triplicate incubations of Gulf of Mexico seep sediment at distinct salinity levels and constant sulfate concentrations. The sulfate concentrations and salinity levels of each incubation are provided in Supplementary Table S1. Full lines and circles represent methane data; dotted lines and triangles signify sulfide data; error bars show standard deviations

also substantial, reaching an average of  $5.3 \text{ nmol/cm}^3$  day after 44 days, or  $\sim 28\%$  that generated by the  $35^\circ\text{C}$  samples. Despite the thermal regime ( $\sim 5^\circ\text{C}$  seafloor sediment) of the inoculum's origin, previous studies have revealed temperature optima for AOM approximately  $5\text{--}10^\circ\text{C}$  above in situ temperatures (Boetius et al., 2009), and, for marine sediment sulfate reduction,  $>20^\circ\text{C}$  above in situ temperatures (Arnosti, Jørgensen, Sagemann, & Thamdrup, 1998; Sagemann, Jørgensen, & Greeff, 1998). In our experiments, heightened rates of overall metabolism associated with higher temperatures (Price & Sowers, 2004) appear to dominate up to  $35^\circ\text{C}$ . Above this temperature, methanotrophic or sulfate reduction-associated enzymes may be compromised, and/or thermophilic constituents of the community may out-compete ANME/SRB for key nutrients (Levén, Eriksson, & Schnürer, 2007). Our observations could also indicate a

decoupling of methane consumption and sulfate reduction (see below), which has been noted at sites of hydrothermal AOM (Kallmeyer & Boetius, 2004).

Between days 44 and 61, sulfide levels of the high-temperature mesocosm samples diminished substantially (Figure 2). This decrease was likely caused by abiotic loss through oxidation with ferric minerals and pyrite formation (Peckmann et al., 2001; Wilkin & Barnes, 1997), and/or by a proliferation of anaerobic sulfide-oxidizing organisms (see “Changes in Microbial Community Composition” section 3.3).

### 3.3 | Changes in microbial community composition

To evaluate changes in the microbial community that may account for the observed sulfide concentrations—and possibly provide

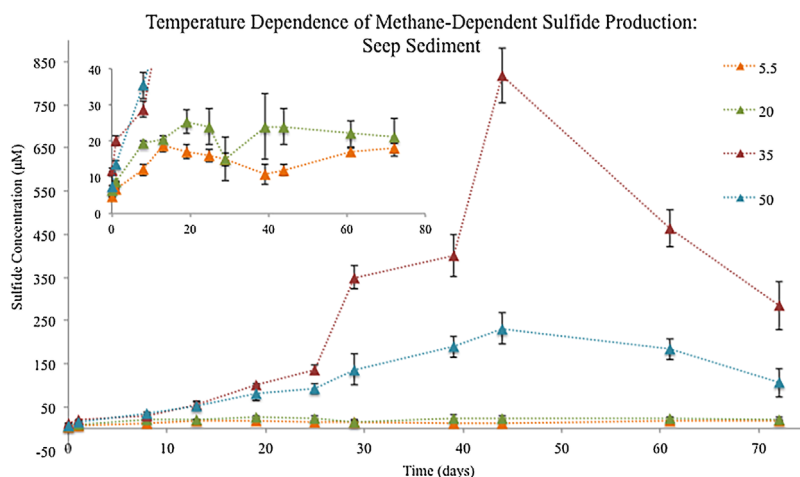


**FIGURE 2** Concentrations of sulfide produced by triplicate batch incubations of methane seep sediment at  $5.5$ ,  $20$ ,  $35$ , and  $50^\circ\text{C}$ . Killed control values were subtracted from each treatment, and error bars show standard deviations

prescriptive insight into shaping complex communities for heightened metabolic activity—16S rRNA gene surveys of five samples (original inoculum sediment at  $T_0$ , 72-day time point samples from 5, 20, 35, and 50 °C seep sediment incubations) were conducted.

The 16S rRNA gene data suggest that, compared with native seep sediment microbial assemblages, more diverse communities exhibit heightened levels of sulfide production at elevated temperatures. Alpha diversity metrics Chao-1 (which estimates species richness) and Inverse Simpson (which incorporates richness and evenness) reveal that heightened sulfide production rates in seep sediment incubations may correlate with both higher relative richness and a greater degree of evenness (Supplementary Table S2), corresponding to a functionally diverse community with many low-abundance constituents. ANME were relatively scarce in the 16S rRNA gene sequence data (<0.1% in all samples), which may seem surprising given the prevalence of sulfide production coupled with methane oxidation at the incubation

scale. However, the Earth Microbiome Project (EMP) primers—used here in order to enable direct comparison with thousands of other studies that have used EMP protocols—have been shown to be relatively ineffective in capturing archaeal 16S sequences in general (Raymann, Moeller, Goodman, & Ochman, 2017), and ANME-2 16S sequences in particular (Case et al., 2015), and future studies targeting these lineages should consider alternate primer sets (Parada, Needham, & Fuhrman, 2016; Timmers, Widjaja-Greefkes, Plugge, & Stams, 2017). To confirm ANME-SRB presence, FISH was performed on 35 °C incubation sediment collected on day 72. Numerous canonical clumped aggregates of ANME-1/2 (Boetius et al., 2000) and *Desulfosarcina/Desulfococcus* (Manz, Eisenbrecher, Neu, & Szewzyk, 1998) were abundant (e.g., field of view provided in Figure 5b). By evaluating the relative abundances of known sulfate reducing and sulfide oxidizing lineages (Supplementary Table S3), we can use community sequencing data to provide insight into the sulfide production

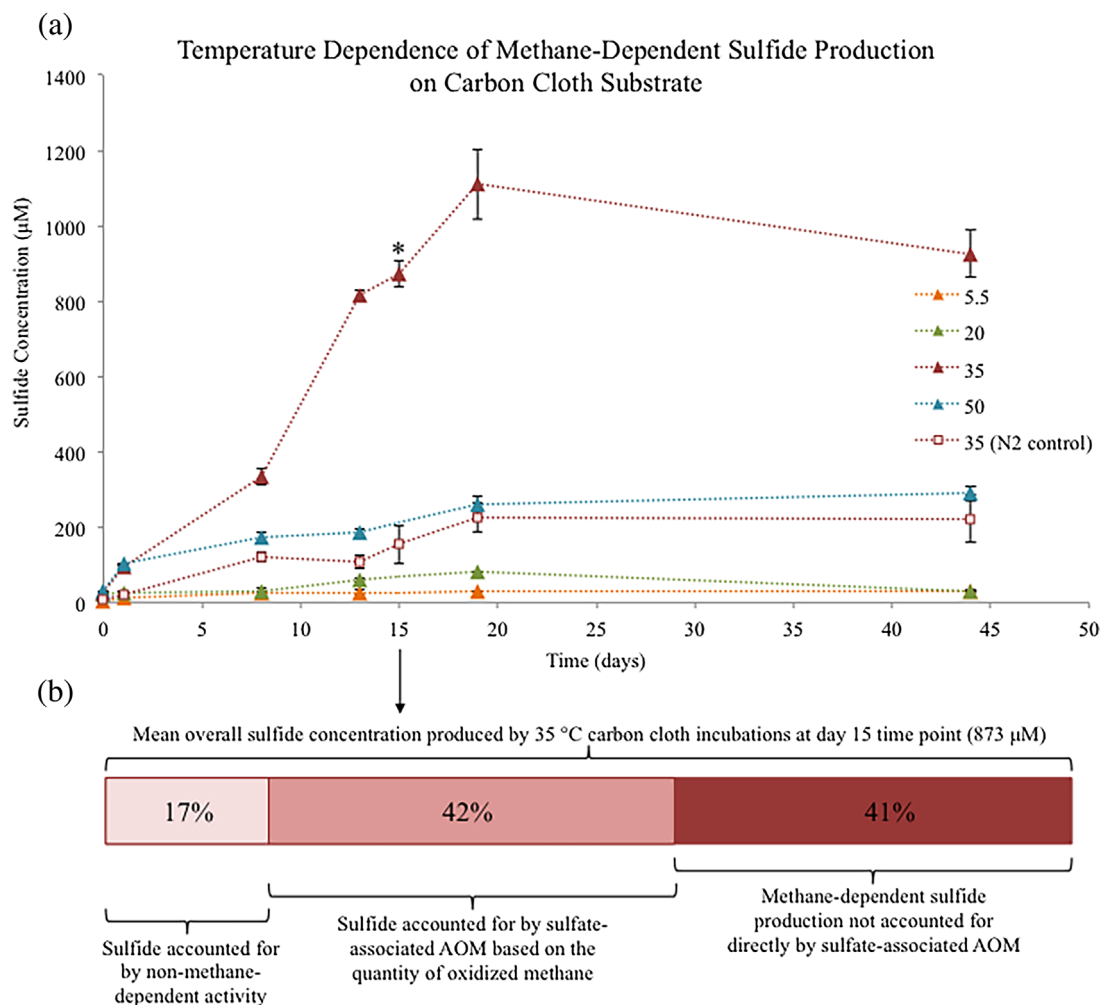


**FIGURE 3** (a) Concentrations of sulfide produced by triplicate batch incubations of carbon cloth at 5.5, 20, 35, and 50 °C. Killed control values were subtracted from each treatment, and error bars show standard deviations. \* = water for D/H analysis was collected. (b) Analysis of methane consumption and sulfide levels of the isothermal methane-free nitrogen control reveal the balance between methane-dependent sulfide production, methane oxidation-linked sulfide production, and non-methane-dependent sulfide production

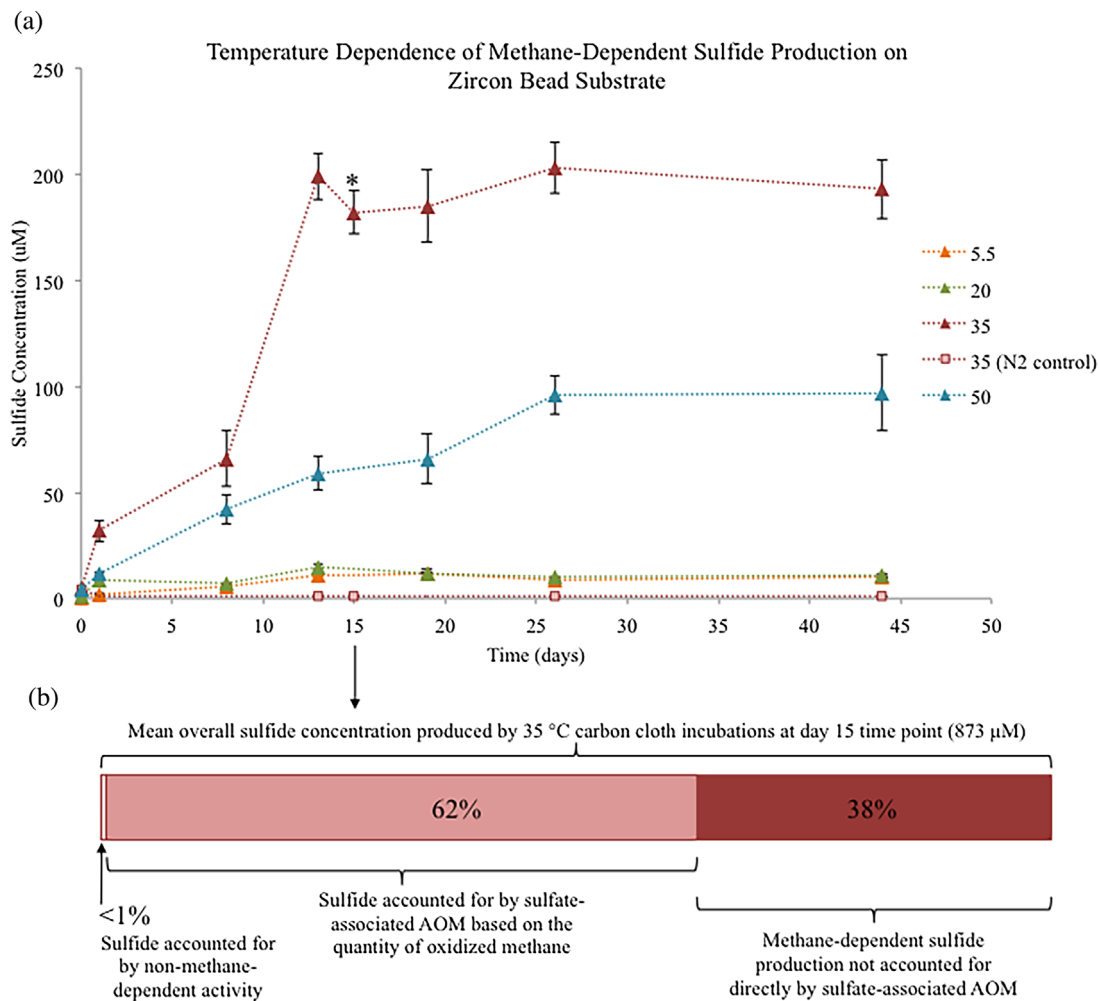


**FIGURE 4** (a) Concentrations of sulfide produced by triplicate batch incubations of zircon beads at 5.5, 20, 35, and 50 °C. Killed control values were subtracted from each treatment, and error bars show standard deviations. \* = water for D/H analysis was collected. (b) Proportions of sulfide at day 15 accounted for by methane-dependent sulfide production, methane oxidation-linked sulfide production, and non-methane-dependent sulfide production

and consumption dynamics observed in the sediment incubations (Figure 2). The presence and abundance of genomic DNA do not directly reveal metabolic activity levels (Maier, Güell, & Serrano, 2009; Muyzer & Stams, 2008). Nonetheless, an organism's abundance does reveal potentially prominent metabolic activities, as higher abundances provide more opportunities for genes to be expressed and associated metabolic reactions—inferred from close cultured representatives or detailed environmental studies—to be enacted. This approach is frequently used to model community function (Bowman, Amaral-Zettler, Rich, Luria, & Ducklow, 2017) and is particularly promising for specific metabolic reactions with few branch points, such as methane and sulfur catabolism (Fierer, 2017; Preheim et al., 2016). The high relative abundance of sequences derived from sulfide oxidizing bacteria (Supplementary Table S2) in the 35 and 50 °C sediment communities, which accounted for 22% (+/- 4% SE) and 28.5% of recovered sequences, respectively (compared with 6.2% from the  $T_0$  inoculum), helps explain the decrease in sulfide concentration between days 44 and

72. The 35 °C condition also had a substantial proportion of sulfate reducing bacteria sequences (12.4% +/- 1.7% SE compared with 7.2% from the  $T_0$  inoculum), consistent with its elevated sulfide production.

### 3.4 | Harnessing AOM on artificial substrates

Establishing a sediment-free, methane oxidizing, sulfide producing microbial community is a strategic priority for the bioenergy industry. Such a capability would enhance the quantity of product per unit volume, lower maintenance costs, and provide a physical scaffold to enrich for specific interspecies communities. Seep sediments are frequently comprised of phyllosilicates transported by fluvial erosion, which can minimize permeability (thereby limiting nutrient inflow and waste removal), adhere to cells, and restrict movement (Hong et al., 2014). AOM also promotes the formation of authigenic carbonates, which may ultimately entomb methane oxidizing constituents (Marlow, Peckmann, & Orphan, 2015).



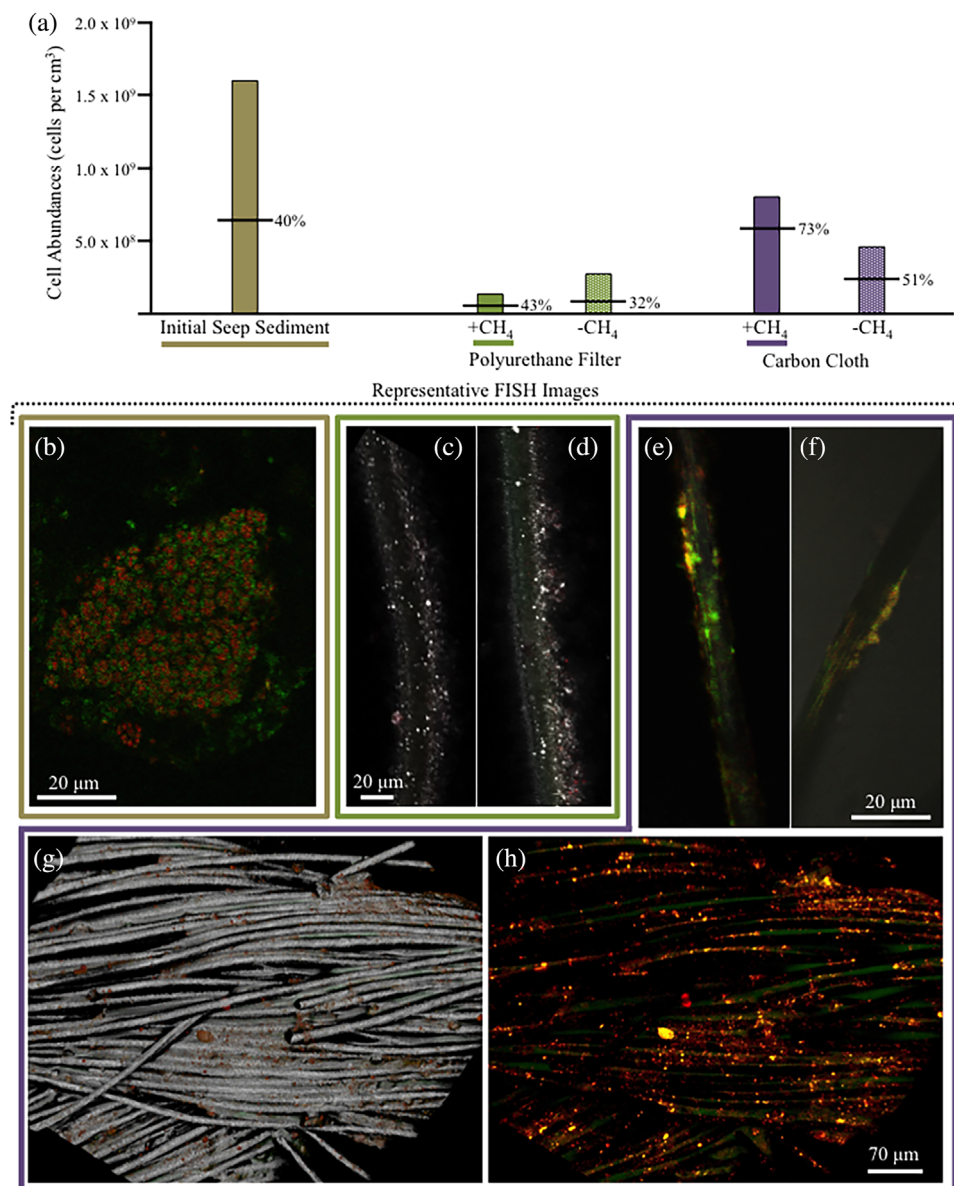


**FIGURE 5** Cell abundances and representative images of microbial communities in seep sediment and adhered to artificial substrates. (a) Cell counts of seep sediment inoculum and from polyurethane filter and carbon cloth surface-associated communities. Incubations lasted 27 days and were conducted with or without methane, as indicated, at 35 °C. Cell abundance values indicate the number of DAPI-visible cells per cm<sup>3</sup>; percentages and partition lines indicate the proportion of DAPI-active cells that were illuminated by the ANME-932 or DSS-658 FISH probes. (b–h) Representative FISH/reflexance images of the respective substrates. (b) Sediment from a 35 °C batch incubation recovered after 72 days. (c–d) Polyurethane filter recovered after 27 days, exhibiting substantial particulate but minimal biomass adherence. (e–h) Carbon cloth from a 35 °C batch incubation recovered after 44 days. Panels e and f show single strands of carbon cloth, with a moderate white light reflectance component in panel f to show the strand outline. Panels g and h show composite images from a 94 μm thick z-stack, with vertical steps of 0.8 μm. Panel G includes a reflectance channel to show the topology of the carbon cloth; the reflectance channel is removed in panel h to reveal sites of successful hybridization. A control sample of unincubated carbon cloth exhibited no probe hybridization (images not shown). See text for microscope parameters. In all images, the FISH probes ANME-932-Cy3 (red stain), and DSS-658-6FAM (green stain) were used; regions of apparent yellow coloration indicate nearly co-localized red and green stains. The scale bar in panel c applies to panels c and d, the scale bar in panel f applies to e and f, and the scale bar in panel h applies to g and h

Here, two artificial substrates were used as potential scaffolds for sediment-free anaerobic methanotrophic communities grown with CH<sub>3</sub>D. Carbon cloth is a permeable, high surface area material shown to promote microbial attachment (Zhang et al., 2012; Zhao et al., 2013) and stimulate direct electron transfer in co-cultures (Chen et al., 2014). Zircon beads offer a non-conductive but topologically suitable surface for microbial

colonization (Scarano, Piattelli, Caputi, Favero, & Piattelli, 2004), and their spherical shapes enable a sediment-like packing structure.

Sulfide production in carbon cloth and zircon bead incubations was monitored over the course of 44 days at 5.5, 20, 35, and 50 °C (Figures 3a and 4a). Carbon cloth incubations produced sulfide at higher rates than corresponding seep sediment incubations. During the

period of peak sulfide production (15 days, Figure 3a), the D/H ratios of the 35 °C incubations' water indicated that 24.2 nmol methane/cm<sup>3</sup> day had been oxidized, accounting for 42% of sulfide production (using the 1:1 stoichiometry of sulfate-associated AOM). Subtracting this component—as well as sulfide produced in the methane-free control (154 μM, or 17%, consistent with other AOM enrichments (Holler et al., 2011) – 41% of overall sulfide production was unaccounted for (Figure 3b). This sulfide was methane-dependent, but did not correspond to a concomitant oxidation of methane; it may have resulted from sulfate reduction linked to oxidation of non-methane organics generated by ANME primary producers. The result signifies an amplification of methane-driven sulfide production useful for downstream technologies that incorporate genetically engineered sulfide oxidizers (Kernan et al., 2016).

Peak sulfide production on zircon bead substrates was substantially lower than in both sediment- and carbon cloth-hosted incubations (Figure 4a). Over the first 13 days of incubation, sulfide production rates in zircon bead-hosted incubations were 15.3 nmol/cm<sup>3</sup> d (35 °C) and 4.5 nmol/cm<sup>3</sup> day (50 °C), or 24% and 32% that of their carbon cloth-hosted counterparts, respectively. In contrast to the carbon cloth incubations, the 35 °C zircon bead-hosted sample exhibited negligible amounts of methane-independent sulfide production (Figure 4b).

Cell abundance counts revealed decreased biomass on both carbon cloth and zircon beads in comparison to sediment-based incubations (Supplementary Table S4): cell abundances in zircon bead incubations were 46.2% ± 15.3% SD that of their sediment-hosted inoculating communities, while carbon cloth incubations hosted 43.2% ± 14.1% SD as many cells. For each temperature condition, zircon bead samples had the highest per-cell sulfide production levels (using maximum sulfide levels attained during the incubations; Supplementary Figure S1). If longer incubation times could enhance biomass while retaining the same per-cell activity, zircon beads may become competitive with carbon cloth as an artificial substrate. However, carbon cloth incubations had a higher proportion of surface-associated cells (69.3% ± 5.1% SD compared with 21.8% ± 8.7% SD for zircon bead incubations; Supplementary Table S4), suggesting a specific adherence that enables easier transferability via substrate rather than a liquid phase. In addition, zircon beads are 11.3 times more dense than carbon cloth, offering diminished sulfide production on a per-mass basis.

To understand which microbial constituents could be responsible for the increased levels of methane oxidation and sulfide production under carbon cloth-associated conditions, 16S rRNA gene surveys were conducted on three 35 °C carbon cloth samples and one 35 °C zircon bead sample. Compared with the 35 °C sediment incubations, the overall community diversity decreased in both carbon cloth (Inv. Simpson from 26.5 to 3) and zircon bead (10.5) incubations (Supplementary Table S2). The relative proportions of known sulfate reducers increased from 12.1% ± 0.9% SE in sediment samples to 66% ± 0.1% SE in carbon cloth- and 19.4% in zircon bead-hosted communities. These results suggest that abstraction of a community from the sediment matrix reduces available niches and promotes dissolved substrate (e.g., sulfate) catabolism.

The 35 °C carbon cloth incubations exhibited a particularly streamlined community: sequences corresponding to *Desulfotomaculum geothermicum* accounted for 55.6% ± 1.5% SE of all recovered sequences, signifying a clear selection for a specific lineage. *D. geothermicum* can utilize a number of organic molecules as electron donors (Daumas, Cord-Ruwisch, & Garcia, 1988), and members of the genus are associated with AOM at the Lost City hydrothermal field (Aullo, Ranchou-Peyruse, Ollivier, & Magot, 2013) and Gulf of Mexico hydrate mounds (Mills, Hodges, Wilson, MacDonald, & Sobocky, 2003). The second most prevalent lineage was an unclassified *Marinobacter* representative, present at 7.9% ± 1.7% SE; these organisms have been implicated in denitrifying hydrocarbon oxidation (Rontani, Mouzdhahir, Michotey, & Bonin, 2002). Microscopic imaging and cell counts using a general DNA stain and an ANME-1/2-specific FISH probe revealed that ANME-1 and/or ANME-2 were relatively prevalent, accounting for an estimated 26.2% ± 8% SE of all microbial constituents in the 35 °C carbon cloth incubations.

### 3.5 | Microscopic analyses reveal distinct ANME-SRB arrangements

Microscopic imaging of sediment and carbon cloth samples using FISH demonstrated distinct spatial associations among SRB and ANME-1 and -2 constituents. In sediment samples, ANME and SRB cells form intermixed consortia in which syntrophy is likely maintained by cytochrome-mediated direct electron transfer (McGlynn, Chadwick, Kempes, & Orphan, 2015). These aggregates were prevalent in 35 °C sediment incubations (Figure 5b). In 35 °C carbon cloth incubations, constituents were observed in association with the surfaces of individual fibers (Figures 5e and 5f). A selected area of carbon cloth with a relatively high microbial load revealed an abundance of SRB and a patchy distribution of ANME-1/2 cells (Figures 5g and 5h). Un-incubated carbon cloth subjected to identical hybridization conditions produced no visible fluorescence signal (data not shown).

The carbon fibers may provide conductive, electron-transferring contact between ANME and SRB, which would preserve the redox-tuned symbiosis but obviate the need for direct contact, thereby enabling more streamlined nutrient delivery and waste removal. The partial segregation between lineages on the carbon cloth, the detection of direct electron transfer between ANME and SRB (McGlynn, Chadwick, Kempes, & Orphan, 2015), as well as previous work revealing carbon cloth as an electron-carrying intermediary for *G. metallireducens* and *M. barkeri* (Chen et al., 2014), make this an intriguing possibility worthy of continued investigation.

### 3.6 | Exploring the properties of artificial substrate adherence and enrichment

While microscopic analysis of the carbon cloth revealed a substantial surface-associated constituency, zircon bead incubations showed abundant organisms in the filtered supernatant but no surface-associated organisms. This observation revealed the importance of (a) textural and/or (b) electrical properties in facilitating ANME-SRB partnerships on artificial

substrates. To assess the relative importance of these two variables, seep sediment was incubated (+/- methane) with carbon cloth and polyurethane filter, which mimics the high porosity and surface area of carbon cloth but is non-conductive. After 27 days of incubation at 35 °C, cell counts revealed a more than fivefold increase in microbial abundance on carbon cloth compared with polyurethane filter under methane-replete conditions (Figure 5a), and negligible quantities of ANME and SRB cells were visible on polyurethane (Figures 5c and 5d). Approximately half of this increase is likely methane-independent (the carbon cloth hosted 1.7 times as many cells than the filter under methane-free conditions), but most of the enhancement was attributable to the addition of methane.

Furthermore, carbon cloth incubations in general, and the methane-rich carbon cloth incubation in particular, favored a selective, substrate-associated enrichment of ANME (ANME-1/2) and SRB (*Desulfosarcina/Desulfococcus*) constituents. While 40% of observed biomass in the inoculum seep sediment consisted of these AOM-implicated lineages—a proportion roughly maintained on the polyurethane filters—51% and 73% of attached cells consisted of these lineages on carbon cloth under methane-free and methane-rich conditions, respectively (Figure 5a). Electrical resistance values confirmed that under incubation conditions, carbon cloth was more than four orders of magnitude more conductive than sediment, zircon beads, and polyurethane filter (Supplementary Table S5). These findings suggest that the electrical conductivity of carbon cloth is a key factor in its capacity to enrich ANME/SRB and enhance methane-fueled sulfide production. Recent microbial fuel cell studies are consistent with this interpretation, as conductive carbon substrates have been used to stimulate electricity generation from methane in ANME enrichments (Chen & Smith, 2018; Ding et al., 2017; Zhao, Ji, Li, & Ren, 2017).

Previous efforts with sediment-free ANME-SRB enrichments have focused largely on the physiological relationships between consortia members (Krukenberg et al., 2016; Laso-Pérez et al., 2016). The resulting mixed cultures can take years to establish and have diminished methane-dependent sulfate reduction rates (Wegener, Krukenberg, Ruff, Kellermann, & Knittel, 2016). Our effort prioritizes enhanced function (methane consumption and methane-dependent sulfide production) and sediment removal over community purity, and offers compelling progress on these fronts. Our analysis shows not only that abstraction from the sediment matrix is possible with a complex AOM-enacting community over the course of weeks rather than years, but that methane-dependent sulfide production per unit volume increases by a factor of 3.5 on the carbon cloth artificial substrate. (This value was calculated using 44-day and 19-day time points and methane-dependent sulfide production coefficients of 0.74 (Figure 1) and 0.83 (Figure 3b), for the 35 °C sediment and carbon cloth incubations, respectively). Harvesting of such uncultivable communities onto artificial substrates is a promising method for expanding the possible functionalities of biotechnological systems.

### 3.7 | Applications of microbially mediated methane activation

The findings presented above signify important developments in the use of methane for bioindustrial practices. Optimized salinity and temperature

conditions inform reactor conditions and set bounds on operational costs. Abstracting AOM activity from the sediment matrix obviates the need for a continuous supply of costly deep-sea inoculum and avoids obstacles to nutrient delivery and fluid flow. Developing an inexpensive medium, devoid of costly organic amendments or electron shuttles, is also beneficial to reducing operating costs. Continued microbial “auto-refinement,” taking advantage of the natural tendency of microbial communities to assemble based on the most efficient metabolism of provided energy sources, will likely yield a highly predictable—and more productive—assemblage for methane bioprocessing.

Once mobilized by uncultivated ANME, methane-derived electrons can be incorporated into a range of systems. SRB have been used for bioremediation (Chardin et al., 2002; García et al., 2001; Hard, Friedrich, & Babel, 1997) and can accumulate intracellular storage molecules (e.g., polyhydroxyalkanoates, or PHAs, Hai, Lange, Rabus, & Steinbüchel, 2004), which are attractive precursors for plastics (Verlinden, Hill, Kenward, Williams, & Radecka, 2007; Wang, Yin, & Chen, 2014). Existing knowledge of PHA metabolic pathways (Aldor & Keasling, 2003; Poblete-Castro et al., 2013) and the genetic tractability of several SRB lineages make enhanced bioplastic production a compelling opportunity, and the direct transfer of methane-derived electrons to SRB would likely increase rates of metabolic activity. Using metabolic products of the ANME-SRB consortium, dissolved inorganic carbon can be mobilized by engineered autotrophs into alcohol fuels (Lan & Liao, 2013) while sulfide could be used as an electron donor to power engineered, chemical-synthesizing strains of sulfide oxidizing bacteria (Kernan et al., 2016). These applications would also limit the atmospheric release of methane, a greenhouse gas with a global warming potential 21 times that of carbon dioxide over a 100-year period.

Despite these opportunities, challenges remain in the design and scale-up of distributed bioreactors. Corrosion associated with unreacted sulfide is a longstanding challenge that has attracted substantial research (e.g., Revie, 2008); in addition to incorporating appropriate reactor materials, avoiding corrosion will require careful tuning of flow rates and metabolic activity within secondary reactors. Initial analysis has demonstrated that using natural gas wells as the reactor can overcome mass transfer obstacles and reach 100% conversion with sufficient reaction rates (Emerson et al., 2017), though such rates were not attained in this study, and the prospects of deploying high-surface area carbon cloth at scale requires further investigation. Nonetheless, the work presented here offers an initial avenue toward rate enhancement per unit volume, and we anticipate that continued improvements of the electrical and physical properties of artificial substrates, as well as incorporation of recently discovered microbial communities oxidizing methane at substantially higher rates (Marlow et al., in prep; Raineault et al., 2017) will bridge the gap.

## 4 | CONCLUSIONS

The availability of methane makes it an attractive target for industrial use, and its high greenhouse warming potential makes its

oxidation appealing for both environmental and economic purposes. Here we provide an approach to harness the methane-oxidizing, sulfide-producing capabilities of microbial communities from marine methane seeps in the service of these dual aims. Microscopic imaging revealed that ANME and SRB were predominant on the carbon cloth substrate, adopted a novel, surface-associated, aggregate-free arrangement, and were selectively enriched compared with native seep sediment (a finding that may be attributable to the electrical conductivity of carbon cloth).

Harnessing complex natural assemblages of organisms offers important advantages over reductionist attempts to engineer model organisms, including metabolic redundancy and an expanded functional space unconstrained by cultivability requirements. Achieving a methane-activating, sulfide-producing mixed culture in a sediment-free context is a key development that presents compelling biotechnological and greenhouse gas mitigation opportunities. On the carbon cloth artificial substrate, sulfide production rates per unit volume increased more than threefold, making the system presented here promising for bioremediating or PHA-producing SRB, or downstream sulfide-utilizing processes. More broadly, this work shows the feasibility of shifting complex microbial communities to tractable systems devoid of the physicochemical challenges of natural substrates. The incorporation of uncultivated, mixed microbial communities into reactor systems will enable practitioners to access an enormous range of biological function for industrial aims, opening a new realm of biotechnological potential.

## ACKNOWLEDGMENTS

We thank Jenny Delaney, Dr. Jason King, Dr. Fauzi Haroon, Dr. Aude Picard, Dr. Daniel Hoer, Dr. Beate Kraft, and Caroline Stetson for experimental assistance and insight on earlier versions of this manuscript. We thank the *Alvin* group and the captains, crew, and science party members aboard the *R/V Atlantis* during the *Alvin* Science Verification Cruise. The information, data, or work presented herein was funded in part by the Advanced Research Projects Agency Energy (ARPA-E), U.S. Department of Energy, under Award Number DE-AR0000433 as well as the National Science Foundation under Grant Number DEB-1542506. Any opinions, findings, and conclusions or recommendations expressed in this material are those of the author(s) and do not necessarily reflect the views of the National Science Foundation.

## ORCID

Jeffrey J. Marlow  <http://orcid.org/0000-0003-2858-8806>

Brandon C. Enalls  <http://orcid.org/0000-0002-5228-1153>

## REFERENCES

Aldor, I. S., & Keasling, J. D. (2003). Process design for microbial plastic factories: Metabolic engineering of polyhydroxyalkanoates. *Current Opinion in Biotechnology*, *14*, 475–483.

- Arnosti, C., Jørgensen, B., Sagemann, J., & Thamdrup, B. (1998). Temperature dependence of microbial degradation of organic matter in marine sediments: Polysaccharide hydrolysis, oxygen consumption, and sulfate reduction. *Marine Ecology Progress Series*, *165*, 59–70.
- Aullo, T., Ranchou-Peyruse, A., Ollivier, B., & Magot, M. (2013). *Desulfotomaculum* spp. and related gram-positive sulfate-reducing bacteria in deep subsurface environments. *Frontiers in Microbiology*, *4*, 362.
- Beal, E. J., Claire, M. W., & House, C. H. (2011). High rates of anaerobic methanotrophy at low sulfate concentrations with implications for past and present methane levels. *Geobiology*, *9*, 131–139.
- Boetius, A., Holler, T., Knittel, K., Felden, J., & Wenzhöfer, F. (2009). Theseabed as natural laboratory: Lessons from uncultivated methanotrophs. In *Uncultivated Microorganisms*. Berlin: Springer, pp. 293–316.
- Boetius, A., Ravensschlag, K., Schubert, C. J., Rickert, D., Widdel, F., Gieseke, A., . . . Pfannkuche, O. (2000). A marine microbial consortium apparently mediating anaerobic oxidation of methane. *Nature*, *407*, 623–626.
- Bowman, J. S., Amaral-Zettler, L. A., Rich, J. J., Luria, C. M., & Ducklow, H. W. (2017). Bacterial community segmentation facilitates the prediction of ecosystem function along the coast of the western Antarctic Peninsula. *The ISME Journal*, *11*, 1460–1471.
- Brandt, A. R., Heath, G., Kort, E., O'sullivan, F., Pétron, G., Jordaan, S., . . . Arent, D. (2014). Methane leaks from North American natural gas systems. *Science*, *343*, 733–735.
- Briones, A., & Raskin, L. (2003). Diversity and dynamics of microbial communities in engineered environments and their implications for process stability. *Current Opinion in Biotechnology*, *14*, 270–276.
- Caporaso, J. G., Lauber, C. L., Walters, W. A., Berg-Lyons, D., Huntley, J., Fierer, N., . . . Bauer, M. (2012). Ultra-high-throughput microbial community analysis on the Illumina HiSeq and MiSeq platforms. *The ISME Journal*, *6*, 1621–1624.
- Caporaso, J. G., Lauber, C. L., Walters, W. A., Berg-Lyons, D., Lozupone, C. A., Turnbaugh, P. J., . . . Knight, R. (2011). Global patterns of 16S rRNA diversity at a depth of millions of sequences per sample. *Proceedings of the National Academy of Sciences*, *108*, 4516–4522.
- Case, D. H., Pasulka, A. L., Marlow, J. J., Grupe, B. M., Levin, L. A., & Orphan, V. J. (2015). Methane seep carbonates host distinct, diverse, and dynamic microbial assemblages. *MBio*, *6*, e01348–e01315.
- Chao, A. (1984). Nonparametric estimation of the number of classes in a population. *Scandinavian Journal of Statistics*, *11*, 265–270.
- Chardin, B., Dolla, A., Chaspoul, F., Fardeau, M., Gallice, P., & Bruschi, M. (2002). Bioremediation of chromate: Thermodynamic analysis of the effects of Cr(VI) on sulfate-reducing bacteria. *Applied Microbiology and Biotechnology*, *60*, 352–360.
- Chen, S., Rotaru, A.-E., Liu, F., Philips, J., Woodard, T. L., Nevin, K. P., & Lovley, D. R. (2014). Carbon cloth stimulates direct interspecies electron transfer in syntrophic co-cultures. *Bioresource Technology*, *173*, 82–86.
- Chen, S., & Smith, A. L. (2018). Methane-driven microbial fuel cells recover energy and mitigate dissolved methane emissions from anaerobic effluents. *Environmental Science: Water Research & Technology*, *4*, 67–79.
- Claassens, N. J., Sousa, D. Z., dos Santos, V. A. M., de Vos, W. M., & Van der Oost, J. (2016). Harnessing the power of microbial autotrophy. *Nature Reviews Microbiology*, *14*, 692–706.
- Cline, J. D. (1969). Pectrophotometric determination of hydrogen sulfide in natural waters. *Limnology and Oceanography*, *14*:454–458.
- Clomburg, J. M., Crumbley, A. M., & Gonzalez, R. (2017). Industrial biomanufacturing: The future of chemical production. *Science*, *355*. <https://doi.org/10.1126/science.aag0804>.
- Coffin, R., Hamdan, L., Plummer, R., Smith, J., Gardner, J., Hagen, R., & Wood, W. (2008). Analysis of methane and sulfate flux in methane-charged sediments from the Mississippi Canyon, Gulf of Mexico. *Marine and Petroleum Geology*, *25*, 977–987.

- Colwell, R. K., & Coddington, J. A. (1994). Estimating terrestrial biodiversity through extrapolation. *Philosophical Transactions of the Royal Society of London. Series B: Biological Sciences*, 345, 101–118.
- Csonka, L. N., & Hanson, A. D. (1991). Prokaryotic osmoregulation: Genetics and physiology. *Annual Reviews in Microbiology*, 45, 569–606.
- Daumas, S., Cord-Ruwisch, R., & Garcia, J. L. (1988). *Desulfotomaculum geothermicum* sp. nov., a thermophilic, fatty acid-degrading, sulfate-reducing bacterium isolated with H<sub>2</sub> from geothermal ground water. *Antonie Van Leeuwenhoek*, 54, 165–178.
- Dekas, A. E., Poretsky, R. S., & Orphan, V. J. (2009). Deep-Sea archaea fix and share nitrogen in methane-consuming microbial consortia. *Science*, 326, 422–426.
- Deutzmann, J. S., & Schink, B. (2011). Anaerobic oxidation of methane in sediments of lake constance, an oligotrophic freshwater lake. *Applied and Environmental Microbiology*, 77, 4429–4436.
- Ding, J., Lu, Y.-Z., Fu, L., Ding, Z.-W., Mu, Y., Cheng, S. H., & Zeng, R. J. (2017). Decoupling of DAMO archaea from DAMO bacteria in a methane-driven microbial fuel cell. *Water Research*, 110, 112–119.
- Edgar, R. C. (2010). Search and clustering orders of magnitude faster than BLAST. *Bioinformatics*, 26, 2460–2461.
- Edgar, R. C. (2013). UPARSE: highly accurate OTU sequences from microbial amplicon reads. *Nature Methods*, 10, 996–998.
- Emerson, D. F., Al Ghatta, A., Woolston, B. M., Fay, A., Kumar, A., & Stephanopoulos, G. (2017). Theoretical analysis of natural gas recovery from marginal wells with a deep well reactor. *AIChE Journal*, 63, 3642–3650.
- Faramawy, S., Zaki, T., & Sakr, A.-E. (2016). Natural gas origin, composition, and processing: A review. *Journal of Natural Gas Science and Engineering*, 34, 34–54.
- Fierer, N. (2017). Embracing the unknown: Disentangling the complexities of the soil microbiome. *Nature Reviews Microbiology*, 15, 579.
- García, C., Moreno, D. A., Ballester, A., Blázquez, M. L., & González, F. (2001). Bioremediation of an industrial acid mine water by metal-tolerant sulphate-reducing bacteria. *Minerals Engineering*, 14, 997–1008.
- Girguis, P. R., Cozen, A. E., & DeLong, E. F. (2005). Growth and population dynamics of anaerobic methane-oxidizing archaea and sulfate-reducing bacteria in a continuous-flow bioreactor. *Applied and Environmental Microbiology*, 71, 3725–3733.
- Girguis, P. R., Orphan, V. J., Hallam, S. J., & DeLong, E. F. (2003). Growth and methane oxidation rates of anaerobic methanotrophic archaea in a continuous-flow bioreactor. *Applied and Environmental Microbiology*, 69, 5472–5482.
- Girvan, M., Campbell, C., Killham, K., Prosser, J., & Glover, L. (2005). Bacterial diversity promotes community stability and functional resilience after perturbation. *Environmental Microbiology*, 7, 301–313.
- Hai, T., Lange, D., Rabus, R., & Steinbüchel, A. (2004). Polyhydroxyalkanoate (PHA) accumulation in sulfate-reducing bacteria and identification of a class III PHA synthase (PhaEC) in *Desulfococcus multivorans*. *Applied and Environmental Microbiology*, 70, 4440–4448.
- Hanson, R. S., & Hanson, T. E. (1996). Methanotrophic bacteria. *Microbiological Reviews*, 60, 439–471.
- Hard, B. C., Friedrich, S., & Babel, W. (1997). Bioremediation of acid mine water using facultatively methylophilic metal-tolerant sulfate-reducing bacteria. *Microbiological Research*, 152, 65–73.
- Haynes, C. A., & Gonzalez, R. (2014). Rethinking biological activation of methane and conversion to liquid fuels. *Nature Chemical Biology*, 10, 331–339.
- Holler, T., Widdel, F., Knittel, K., Amann, R., Kellermann, M. Y., Hinrichs, K.-U., ... Wegener, G. (2011). Thermophilic anaerobic oxidation of methane by marine microbial consortia. *ISME J*, 5, 1946–1956.
- Hong, Z., Zhao, G., Chen, W., Rong, X., Cai, P., Dai, K., & Huang\*, Q. (2014). Effects of solution chemistry on bacterial adhesion with phyllosilicates and goethite explained by the extended DLVO theory. *Geomicrobiology Journal*, 31, 419–430.
- Howarth, R. W. (2014). A bridge to nowhere: Methane emissions and the greenhouse gas footprint of natural gas. *Energy Science & Engineering*, 2, 47–60.
- Hunter, P. R., & Gaston, M. A. (1988). Numerical index of the discriminatory ability of typing systems: An application of Simpson's index of diversity. *Journal of Clinical Microbiology*, 26, 2465–2466.
- Joo, J. O., Choi, J., Kim, I. H., Kim, Y., & Oh, B. (2015). Effective bioremediation of Cadmium (II), nickel (II), and chromium (VI) in a marine environment by using *Desulfovibrio desulfuricans*. *Biotechnology and Bioprocess Engineering: BBE*, 20, 937.
- Joye, S. B., Boetius, A., Orcutt, B. N., Montoya, J. P., Schulz, H. N., Erickson, M. J., & Lugo, S. K. (2004). The anaerobic oxidation of methane and sulfate reduction in sediments from Gulf of Mexico cold seeps. *Chemical Geology*, 205, 219–238.
- Kadam, P. C., Ranade, D., Mandelco, L., & Boone, D. R. (1994). Isolation and characterization of *Methanoblobus bombayensis* sp. nov., a methylophilic methanogen that requires high concentrations of divalent cations. *International Journal of Systematic and Evolutionary Microbiology*, 44, 603–607.
- Kallmeyer, J., & Boetius, A. (2004). Effects of temperature and pressure on sulfate reduction and anaerobic oxidation of methane in hydrothermal sediments of guaymas basin. *Applied and Environmental Microbiology*, 70, 1231–1233.
- Kernan, T., Majumdar, S., Li, X., Guan, J., West, A. C., & Banta, S. (2016). Engineering the iron-oxidizing chemolithoautotroph *Acidithiobacillus ferrooxidans* for biochemical production. *Biotechnology and Bioengineering*, 113, 189–197.
- Kernan, T., West, A. C., & Banta, S. (2017). Characterization of endogenous promoters for control of recombinant gene expression in *Acidithiobacillus ferrooxidans*. *Biotechnology and Applied Biochemistry*, 64, 793–802.
- Kleindienst, S., Herbst, F.-A., Stagars, M., von Netzer, F., von Bergen, M., Seifert, J., ... Knittel, K. (2014). Diverse sulfate-reducing bacteria of the *Desulfosarcina/Desulfococcus* clade are the key alkane degraders at marine seeps. *ISME J*, 8, 2029–2044.
- Kolmert, A., Wikström, P., & Hallberg, K. B. (2000). A fast and simple turbidimetric method for the determination of sulfate in sulfate-reducing bacterial cultures. *Journal of Microbiological Methods*, 41, 179–184.
- Krüger, M., Wolters, H., Gehre, M., Joye, S. B., & Richnow, H. (2008). Tracing the slow growth of anaerobic methane-oxidizing communities by 15N-labelling techniques. *FEMS Microbiology Ecology*, 63, 401–411.
- Krukenberg, V., Harding, K., Richter, M., Glöckner, F. O., Gruber-Vodicka, H. R., Adam, B., ... Wegener, G. (2016). *Candidatus Desulfofervidus auxilii*, a hydrogenotrophic sulfate-reducing bacterium involved in the thermophilic anaerobic oxidation of methane. *Environmental Microbiology*, 18, 3073–3091.
- Lan, E. I., & Liao, J. C. (2013). Microbial synthesis of n-butanol, isobutanol, and other higher alcohols from diverse resources. *Bioresource Technology*, 135, 339–349.
- Laso-Pérez, R., Wegener, G., Knittel, K., Widdel, F., Harding, K. J., Krukenberg, V., ... Musat, F. (2016). Thermophilic archaea activate butane via alkyl-coenzyme M formation. *Nature*, 539, 396–401.
- Levén, L., Eriksson, A. R., & Schnürer, A. (2007). Effect of process temperature on bacterial and archaeal communities in two methanogenic bioreactors treating organic household waste. *FEMS Microbiology Ecology*, 59, 683–693.
- Lloyd, K. G., Albert, D. B., Biddle, J. F., Chanton, J. P., Pizarro, O., & Teske, A. (2010). Spatial structure and activity of sedimentary microbial communities underlying a *Beggiatoa* spp. mat in a Gulf of Mexico hydrocarbon seep. *PLoS ONE*, 5:e8738.
- Maier, T., Güell, M., & Serrano, L. (2009). Correlation of mRNA and protein in complex biological samples. *FEBS Letters*, 583, 3966–3973.
- Manz, W., Eisenbrecher, M., Neu, T. R., & Szewzyk, U. (1998). Abundance and spatial organization of Gram-negative sulfate-reducing bacteria in

- activated sludge investigated by in situ probing with specific 16S rRNA targeted oligonucleotides. *FEMS Microbiology Ecology*, 25, 43–61.
- Marlow, J. J., Steele, J. A., Ziebis, W., Thurber, A. R., Levin, L. A., & Orphan, V. J. (2014). Carbonate-hosted methanotrophy represents an unrecognized methane sink in the deep sea. *Nature Communications*, 5, 5094–5106.
- Marlow, J., Peckmann, J., & Orphan, V. (2015). Autoendoliths: A distinct type of rock-hosted microbial life. *Geobiology*, 13, 303–307.
- Marlow, J., Gartman, A., Jungbluth, S., Hoer, D., Reynard, L., Tuross, N., ... Girguis, P. (2018). Rock-hosted microbial communities possess substantial methane oxidizing potential at geologically diverse methane seep sites. Abstract BN24C-1096, Ocean Sciences Meeting, Portland, OR, 12–16 Feb.
- Marlow, J. J., Steele, J. A., Case, D. H., Connon, S. A., Levin, L. A., & Orphan, V. J. (2014). Microbial abundance and diversity patterns associated with sediments and carbonates from the methane seep environments of Hydrate Ridge, OR. *Frontiers in Marine Science*, 1, 44.
- Marlow, J. J., Steele, J. A., Ziebis, W., Scheller, S., Case, D., Reynard, L. M., & Orphan, V. J. (2017). Monodeuterated methane, an isotopic tool to assess biological methane metabolism rates. ed. susannah timmers green tringe peer treude, tina. *mSphere*, 2. <http://doi.org/10.1002/bit.26576>
- McAnulty, M. J., Poosarla, V. G., Li, J., Soo, V. W., Zhu, F., & Wood, T. K. (2017). Metabolic engineering of *Methanosarcina acetivorans* for lactate production from methane. *Biotechnology and Bioengineering*, 114, 852–861.
- McGlynn, S. E., Chadwick, G. L., Kempes, C. P., & Orphan, V. J. (2015). Single cell activity reveals direct electron transfer in methanotrophic consortia. *Nature*, 526, 531–535.
- Mills, H. J., Hodges, C., Wilson, K., MacDonald, I. R., & Sobczyk, P. A. (2003). Microbial diversity in sediments associated with surface-breaching gas hydrate mounds in the Gulf of Mexico. *FEMS Microbiology Ecology*, 46, 39–52.
- Muyzer, G., & Stams, A. J. (2008). The ecology and biotechnology of sulphate-reducing bacteria. *Nature Reviews Microbiology*, 6, 441–454.
- Nauhaus, K., Albrecht, M., Elvert, M., Boetius, A., & Widdel, F. (2007). In vitro cell growth of marine archaeal-bacterial consortia during anaerobic oxidation of methane with sulfate. *Environmental Microbiology*, 9, 187–196.
- Nazem-Bokaei, H., Gopalakrishnan, S., Ferry, J. G., Wood, T. K., & Maranas, C. D. (2016). Assessing methanotrophy and carbon fixation for biofuel production by *Methanosarcina acetivorans*. *Microbial cell factories*, 15, 10.
- Nybo, S. E., Khan, N. E., Woolston, B. M., & Curtis, W. R. (2015). Metabolic engineering in chemolithoautotrophic hosts for the production of fuels and chemicals. *Metabolic Engineering*, 30, 105–120.
- Orphan, V. J., Orphan, V. J., Ussler III, W., Naehr, T. H., House, C. H., Hinrichs, K. U., & Paull, C. K. (2004). Geological, geochemical, and microbiological heterogeneity of the seafloor around methane vents in the Eel River Basin, offshore California. *Chemical Geology*, 205, 265–289.
- Parada, A. E., Needham, D. M., & Fuhrman, J. A. (2016). Every base matters: Assessing small subunit rRNA primers for marine microbiomes with mock communities, time series and global field samples. *Environmental Microbiology*, 18, 1403–1414.
- Pasulka, A. L., Levin, L. A., Steele, J. A., Case, D. H., Landry, M. R., & Orphan, V. J. (2016). Microbial eukaryotic distributions and diversity patterns in a deep-sea methane seep ecosystem. *Environmental Microbiology*, 18, 3022–3043.
- Peckmann, J., Reimer, A., Luth, U., Luth, C., Hansen, B., Heinicke, C., ... Reitner, J. (2001). Methane-derived carbonates and authigenic pyrite from the northwestern Black Sea. *Marine Geology*, 177, 129–150.
- Pfeffer, C., Larsen, S., Song, J., Dong, M., Besenbacher, F., Meyer, R. L., ... El-Naggar, M. Y. (2012). Filamentous bacteria transport electrons over centimetre distances. *Nature*, 491, 218–221.
- Poblete-Castro, I., Binger, D., Rodrigues, A., Becker, J., dos Santos, V. A. M., & Wittmann, C. (2013). In-silico-driven metabolic engineering of *Pseudomonas putida* for enhanced production of poly-hydroxyalkanoates. *Metabolic Engineering*, 15, 113–123.
- Preheim, S. P., Olesen, S. W., Spencer, S. J., Materna, A., Varadharajan, C., Blackburn, M., ... Alm, E. J. (2016). Surveys, simulation and single-cell assays relate function and phylogeny in a lake ecosystem. *Nature Microbiology*, 1, 16130.
- Price, P. B., & Sowers, T. (2004). Temperature dependence of metabolic rates for microbial growth, maintenance, and survival. *Proceedings of the National Academy of Sciences of the United States of America*, 101, 4631–4636.
- Raineault, N., Girguis, P., Auscavitch, S., Castillo, C., Lubetkin, M., Marlow, J., ... Kane, R. (2017). Exploration of central California basins, cold seeps, and san juan seamount. *Oceanography*, 30, 36–37.
- Raymann, K., Moeller, A. H., Goodman, A. L., & Ochman, H. (2017). Susannah green tringe. *mSphere 2 Unexplored archaeal diversity in the great ape gut microbiome*. <http://msphere.asm.org/content/2/1/e00026-17.abstract>
- Revie, R. W. (2008). Kinetics: polarization and corrosion rates, *Corrosion and corrosion control: an introduction to corrosion science and engineering* (pp. 53–82), Hoboken: John Wiley & Sons.
- Rontani, J.-F., Mouzdahir, A., Michotey, V., & Bonin, P. (2002). Aerobic and anaerobic metabolism of squalene by a denitrifying bacterium isolated from marine sediment. *Archives of Microbiology*, 178, 279–287.
- RTL Genomics. (2016). Data Analysis Methodology, Version 2.3.1. RTL Genomics. [https://static1.squarespace.com/static/5807c0ce579fb39e1dd6add/t/5813af0fd482e97e5eb4fcb5/1477685010205/Data\\_Analysis\\_Methodology.pdf](https://static1.squarespace.com/static/5807c0ce579fb39e1dd6add/t/5813af0fd482e97e5eb4fcb5/1477685010205/Data_Analysis_Methodology.pdf).
- Ruff, S. E., Biddle, J. F., Teske, A. P., Knittel, K., Boetius, A., & Ramette, A. (2015). Global dispersion and local diversification of the methane seep microbiome. *Proceedings of the National Academy of Sciences*, 112, 201421865.
- Sagemann, J., Jørgensen, B. B., & Greeff, O. (1998). Temperature dependence and rates of sulfate reduction in cold sediments of svalbard, arctic ocean. *Geomicrobiology Journal*, 15, 85–100.
- Scarano, A., Piattelli, M., Caputi, S., Favero, G. A., & Piattelli, A. (2004). Bacterial adhesion on commercially pure titanium and zirconium oxide disks: An in vivo human study. *Journal of Periodontology*, 75, 292–296.
- Scheller, S., Yu, H., Chadwick, G. L., McGlynn, S. E., & Orphan, V. J. (2016). Artificial electron acceptors decouple archaeal methane oxidation from sulfate reduction. *Science*, 351, 703–707.
- Shank, T. M., Hsing, P., Carney, R. S., Herrera, S., Heyl, T., Munro, C., ... EPotter, J. (2012). Exploration and Discovery of Hydrocarbon Seeps, Coral Ecosystems, and Shipwrecks in the Deep Gulf of Mexico. In *AGU Fall Meeting Abstracts*.
- Simpson, E. H. (1949). Measurement of diversity. *Nature*, 163, 688.
- Smemo, K. A., & Yavitt, J. B. (2007). Evidence for anaerobic CH<sub>4</sub> oxidation in freshwater peatlands. *Geomicrobiology Journal*, 24, 583–597.
- Soo, V. W., McAnulty, M. J., Tripathi, A., Zhu, F., Zhang, L., Hatzakis, E., ... Gopalakrishnan, S. (2016). Reversing methanogenesis to capture methane for liquid biofuel precursors. *Microbial Cell Factories*, 15, 1.
- Stams, A. J. M., Van Dijk, J. B., Dijkema, C., & Plugge, C. M. (1993). Growth of syntrophic propionate-Oxidizing bacteria with fumarate in the absence of methanogenic bacteria. *Applied and Environmental Microbiology*, 59, 1114–1119.
- Stocker, T. (2014). *Climate change 2013: the physical science basis: Working Group I contribution to the Fifth assessment report of the Intergovernmental Panel on Climate Change*. Cambridge University Press.
- Sublette, K. L., & Sylvester, N. D. (1987). Oxidation of hydrogen sulfide by *Thiobacillus denitrificans*: Desulfurization of natural gas. *Biotechnology and Bioengineering*, 29, 249–257.
- Takenaka, S., Kobayashi, S., Ogihara, H., & Otsuka, K. (2003). Ni/SiO<sub>2</sub> catalyst effective for methane decomposition into hydrogen and carbon nanofiber. *Journal of Catalysis*, 217, 79–87.

- Tang, P., Zhu, Q., Wu, Z., & Ma, D. (2014). Methane activation: The past and future. *Energy & Environmental Science*, 7, 2580–2591.
- Timmers, P. H., Suarez-Zuluaga, D. A., van Rossem, M., Diender, M., Stams, A. J., & Plugge, C. M. (2016). Anaerobic oxidation of methane associated with sulfate reduction in a natural freshwater gas source. *ISME Journal*, 10, 1400–1412.
- Timmers, P. H., Widjaja-Greefkes, H. A., Plugge, C. M., & Stams, A. J. (2017). Evaluation and optimization of PCR primers for selective and quantitative detection of marine ANME subclusters involved in sulfate-dependent anaerobic methane oxidation. *Applied Microbiology and Biotechnology*, 101, 1–13.
- Treude, T., Boetius, A., Knittel, K., Wallmann, K., & Jorgensen, B. (2003). Anaerobic oxidation of methane above gas hydrates at Hydrate Ridge, NE Pacific Ocean. *Marine Ecology Progress Series*, 264, 1–14.
- Treude, T., Orphan, V., Knittel, K., Gieseke, A., House, C. H., & Boetius, A. (2007). Consumption of methane and CO<sub>2</sub> by methanotrophic microbial mats from gas seeps of the anoxic black sea. *Applied and Environmental Microbiology*, 73, 2271–2283.
- Trotsenko, Y. A., & Murrell, J. C. (2008). Metabolic Aspects of Aerobic Obligate Methanotrophy\*. In: *Advances in Applied Microbiology*. Academic Press, Vol. Volume 63 183–229. <http://www.sciencedirect.com/science/article/pii/S0065216407000056>
- U.S. Energy Information Administration. (2016). Gross Natural Gas Production. [www.eia.gov](http://www.eia.gov)
- Verlinden, R. A., Hill, D. J., Kenward, M., Williams, C. D., & Radecka, I. (2007). Bacterial synthesis of biodegradable polyhydroxyalkanoates. *Journal of Applied Microbiology*, 102, 1437–1449.
- Wang, Y., Yin, J., & Chen, G.-Q. (2014). Polyhydroxyalkanoates, challenges and opportunities. *Current Opinion in Biotechnology*, 30, 59–65.
- Wegener, G., Krukenberg, V., Riedel, D., Tegetmeyer, H. E., & Boetius, A. (2015). Intercellular wiring enables electron transfer between methanotrophic archaea and bacteria. *Nature*, 526, 587–590.
- Wegener, G., Krukenberg, V., Ruff, S. E., Kellermann, M. Y., & Knittel, K. (2016). Metabolic capabilities of microorganisms involved in and associated with the anaerobic oxidation of methane. *Frontiers in Microbiology*, 7, 46.
- Wegener, G., Shovitri, M., Knittel, K., Niemann, H., Hovland, M., & Boetius, A. (2008). Biogeochemical processes and microbial diversity of the Gullfaks and Tommeliten methane seeps (Northern North Sea). *Biogeosciences, Discussions* 5: 971–1015.
- Weisburg, W. G., Barns, S. M., Pelletier, D. A., & Lane, D. J. (1991). 16S ribosomal DNA amplification for phylogenetic study. *Journal of Bacteriology*, 173, 697–703.
- Wilkin, R., & Barnes, H. (1997). Formation processes of framboidal pyrite. *Geochimica et Cosmochimica Acta*, 61, 323–339.
- York, A. P., Xiao, T., & Green, M. L. (2003). Brief overview of the partial oxidation of methane to synthesis gas. *Topics in Catalysis*, 22, 345–358.
- Zhang, D., Zhu, W., Tang, C., Suo, Y., Gao, L., Yuan, X., ... Cui, Z. (2012). Bioreactor performance and methanogenic population dynamics in a low-temperature (5–18°C) anaerobic fixed-bed reactor. *Bioresource Technology*, 104, 136–143.
- Zhao, H., Li, J., Li, J., Yuan, X., Piao, R., Zhu, W., ... Cui, Z. (2013). Organic loading rate shock impact on operation and microbial communities in different anaerobic fixed-bed reactors. *Bioresource Technology*, 140, 211–219.
- Zhao, Q., Ji, M., Li, R., & Ren, Z. J. (2017). Long-term performance of sediment microbial fuel cells with multiple anodes. *Bioresource Technology*, 237, 178–185.

## SUPPORTING INFORMATION

Additional Supporting Information may be found online in the supporting information tab for this article.

**How to cite this article:** Marlow JJ, Kumar A, Enalls BC, et al. Harnessing a methane-fueled, sediment-free mixed microbial community for utilization of distributed sources of natural gas. *Biotechnology and Bioengineering*. 2018;115: 1450–1464. <https://doi.org/10.1002/bit.26576>